FORSCHUNGSZENTRUM
ROSSENDORF e.V.

FZR

FZR-124
February 1996

Vladimir Kolevzon

Surface Light Scattering Spectroscopy of the Gallium Liquid-Vapor Interface

Forschungszentrum Rossendorf e.V.
Postfach 51 01 19 · D-01314 Dresden
Bundesrepublik Deutschland

Telefon (0351) 260 2422
Telefax (0351) 260 3484
E-Mail kolevzon@fz-rossendorf.de

Contents

Surface Light Scattering Spectroscopy of the Gallium Liquid-Vapor Interface

Vladimir Kolevzon

Abstract

High frequency capillary waves at liquid Ga surface have been studied by means of quasi-elastic light scattering spectroscopy. The observed frequencies and damping constants of waves differed greatly from classical theoretical treatment of liquid Ga surface as that of a simple liquid. This effect was explained due to the presence of the surface layer, possessing visco-elastic properties extracted, for the first time, from the fit of experimental spectra with an appropriate theoretical form. Negative value of the surface dilational viscosity has been derived for all wavenumbers studied. At high wavenumbers q the wave dispersion behavior is best likely linked to the weak coupling between dilational and capillary modes, while at low and moderate q the experimental data resemble to the mixed oscillations. This behavior is consistent with an influence of diffusion and adsorption on the waves propagation.

1 Introduction

Quasi-elastic light scattering from thermally excited capillary waves (or *ripplons*) on liquid surfaces becomes a powerful technique for studying different interfaces [1, 2]. This method is applicable when most of the classical techniques fail because of their invasive character. A large number of pure transparent liquids have been studied up to now and an excellent agreement with theoretical predictions, based on the hydrodynamic theory was achieved.

Large deviations have been found only for the liquid metal, in particular mercury, [3]. An attempt to explain such anomalies has been made in [4] by using the idea of surface coverage by a monolayer of nonmetallic atoms. The monolayer, possessing visco-elastic properties (see below) has great influence on the capillary waves propagation. Up to now there is no strict theoretical basis for two interfacial viscosities. In the hydrodynamic approach these viscosities are introduced as dissipative parts of the surface moduli, using the functions of linear response [5]. Such treatment may be ill-defined on the molecular level, where the kinetic processes of mass interchange are most important but in fact are hidden into the hydrodynamic limit.

At the same time, some theoretical papers, making use of statistical pseudopotential models, predict an oscillatory density profile of liquid metal-vapor interface [6]. These papers postulated the existence of a highly correlated liquid metal-vapor zone with a characteristic size of a few atomic diameter into the bulk. Two resent experimental studies, using X-ray reflectivity, confirm this theoretical prediction and clearly demonstrate surface layering in mercury and liquid gallium [7, 8]. The physical nature of these layers is not clear up to now: they are formed either by metallic atoms or nonmetallic ones, adsorbed on the liquid metal surface from the gas phase.

Despite of the seeming simplicity of the proposed experimental method, the light scattering is evidently a very sensitive tool to probe a liquid metal surface, even using a phenomenological model for description of the interfacial processes. On the other hand there is a possibility to judge upon the validity of the hydrodynamical model in application to thin film on the liquid metal surface what has been never considered before to our knowledge. Independent from its physical structure, the liquid metal-vapor interface might be considered as a quasi two-dimensional film, compressible in the plane parallel to the interface and incompressible normal to it. Surface film viscoelasticity affects the propagation of the surface capillary waves which makes it possible to detect those film properties experimentally. The present study applies the light scattering spectroscopy mainly to a free surface of liquid gallium.

2 Theoretical background

A liquid surface is subjected to continuous disturbances on the molecular level. These disturbances appear in form of capillary waves which in turn are present due to random pressure fluctuation in the liquid bulk. The surface tension plays a role of a restoring force for short-length capillary waves which are damped by the bulk viscosity. The linearized Navier-Stokes equation gives the dispersion equation for capillary waves propagation $D(\omega) = 0$, where the complex frequency $\omega = \omega_0 + i \cdot \Gamma$ is connected with the wavenumber q via [9]

$$(\omega + 2\nu q^2)^2 + \gamma_0 q^3 \rho = 4\nu^2 q^2 \sqrt{1 + \omega/\nu q^2}, \tag{1}$$

where γ_0 is the surface tension, and ν the kinematic viscosity. $\omega_0$and Γ are the temporal frequency and the damping coefficient of the waves, respectively. When the dispersion equation has complex roots it corresponds to the propagating regime of capillary waves. If the roots are pure imaginary the modes are overdamped. Which branch is the dominating one depends strongly on the physical properties of the fluid, namely the surface tension and the kinematic viscosity. The capillary modes at the surface of liquid metals and of all transparent fluids with moderate viscosity are always found in the propagating regime. In the first order approximation to the solution of equation (1) the frequency and damping coefficient are expressed as [9]:

$$\begin{aligned} \omega_0 &= \sqrt{\gamma_0 q^3/\rho} && (2) \\ \Gamma &= \nu q^2 && (3) \end{aligned}$$

Light scattering from capillary wave have has been extensively considered in ([1] and references there), therefore only the results will be summarized here. Capillary waves scatter light mainly around zero scattering angle with the scattered intensity $I_s \sim 1/\gamma_0 q^2$. The power spectrum of light scattered by a wave with wavenumber q is approximately given by the Lorentzian shape [1]:

$$P(\omega) = \frac{kT}{\pi\gamma_0}\frac{\eta}{\rho}\frac{1}{(\omega-\omega_0)^2+\Gamma^2} \qquad (4)$$

where w is real and peak frequency corresponds to ω_0, the half width to Γ.

It has been suggested [10] that the monolayer visco-elasticity may be described by two kinds of stress: shear and dilation. Each of them involves an elastic and a viscous part. The surface tension γ_0 and the shear viscosity γ' (normal to the interface) are included into a shear modulus:

$$\gamma(\omega) = \gamma_0 + i\omega\gamma' \qquad (5)$$

The dilational modulus can be written as the superposition of the surface elasticity and dilational viscosity:

$$\epsilon(\omega) = \epsilon_0 + \imath\omega\epsilon' \qquad (6)$$

For a monolayer covered liquid surface, possessing visco-elastic properties, the capillary wave propagation is affected by these properties and the dispersion equation written in dimensionless form is [5, 1]

$$D(s) = s^2[(s+1)^2 + y - \sqrt{2s+1}] + (\alpha y + \beta s)[s^2\sqrt{2s+1} + (y+\delta s)(\sqrt{2s+1}-1)] + \delta s^3 \qquad (7)$$

where $s = -i\omega\tau_0, \tau_0 = \rho/2\eta q^2, y = \gamma_0\rho/4\eta^2 q, \alpha = \epsilon_0/\gamma_0, \beta = \epsilon' q/2\eta, \delta = \gamma' q/2\eta$

The theoretical spectrum for thermally exited capillary waves on monolayer covered liquid surface is well known and can be expressed as [1]

$$P(\omega) = \frac{kT}{\omega}\frac{\tau_0 q}{\rho} Im[\frac{s^2 + (\alpha y + \beta s)[\sqrt{2s+1} - 1]}{D(s)}] \tag{8}$$

3 Experimental technique

The main goal of light scattering spectroscopy is to get values of ω_0 and Γ for capillary waves of fixed q. A single wave of wavenumber q scatters light at a well defined angle δq with direction of the mirror reflection.

Due to inelastic interaction of scattered light with a selected capillary wave the frequency of light is Doppler-shifted but the scattered intensity is very low. Therefore, the Heterodyne light beat spectroscopy [12] is necessary: its high resolution allows detection of small signals and low frequency shifts. The scattered light with electric field amplitude E_s is mixed with a reference beam E_r (ideally time-independent), coming into the same direction. The frequency of the resulting signal is equal to the difference of the two frequencies. The output photocurrent is given by:

$$I(t) \sim |E_r|^2 + |E_s|^2 + 2Re(E_r^* E_s exp(i(\omega_r - \omega s)t) \tag{9}$$

so that $I(t)$ consists of a d.c. component (in ideal case) plus a heterodyne-beat term at the Doppler-shifted frequency.

The experimental set-up is shown in Figure 1. Presently built optical system is based on the well known configuration described in [2]: a beam from a 5 mW He-Ne laser ($TEM_{00}, \lambda = 632.5nm$, Melles-Griot) was spatially filtered and then focused at a photodetector using a two lens system. The beam traveling horizontally is tilted by the mirror and falls on the liquid surface at an angle approx. 10° to diminish the influence of the surface curvature. The light scattered by surface waves is mixed with a reference beam which arises from the image of a diffraction grating on the liquid surface. Each reference beam is thus found to be spatially coherent with the scattered one. Far from the liquid surface the diffracted beams are sufficiently separated and each spot is selected by the pinhole preceded an avalanche photodiode.

The diffraction grating, as a source of reference beams, was produced using a vapor-deposited Cr-mask on a glass substrate. To be sure that scattering arises from the main order beam the grating has to be "weak" in the sense that the maximum light power concentrated at zero order and the intensities of all higher orders should be reduced as much as possible. Therefore, an additional grating having "black" elements from iron oxide with three times lower optical density than the Cr elements has been used. The reflection conditions at different liquid surfaces require an alteration of the E_r/E_s ratio. On the one side $E_s \sim 1/\gamma_0$ on the other hand E_s is proportional to the reflection coefficient. Because the surface tension of liquid gallium is ten times higher than that of water, and the reflection coefficient is 15-20 times more, the scattering power expected to be even more then for water. But the reference beam, reflected by liquid Ga, is much stronger, thus the reference beam intensity has to be adjusted. The most suitable way for it is to use a set of optical filters with low optical densities, if made on a thin film the beam distortion is negligible.

The signal out-coming from an avalanche module (avalanche photodiode+preamplifier, Hamamatsu) was fed to a Spectrum Analyzer (ROCKLAND) where the averaged power spectrum was acquired during the time less than 20s. The reason for the choice of an avalanche photodiode instead of a traditional photomultiplier was to avoid saturation problems under enhanced amount of light. It was established [2] that in case of the heterodyne technique the shot noise, depending on the signal amplitude, gives the main contribution to the photodetector noise. It has been also shown [13] that signal-to-noise ratio is better for a photodiode, having larger quantum efficiency, than that for a photomultiplier when the light power is growing. The ripplon wavenumber has been determined from a photo of the diffraction spots taken with a CCD camera.

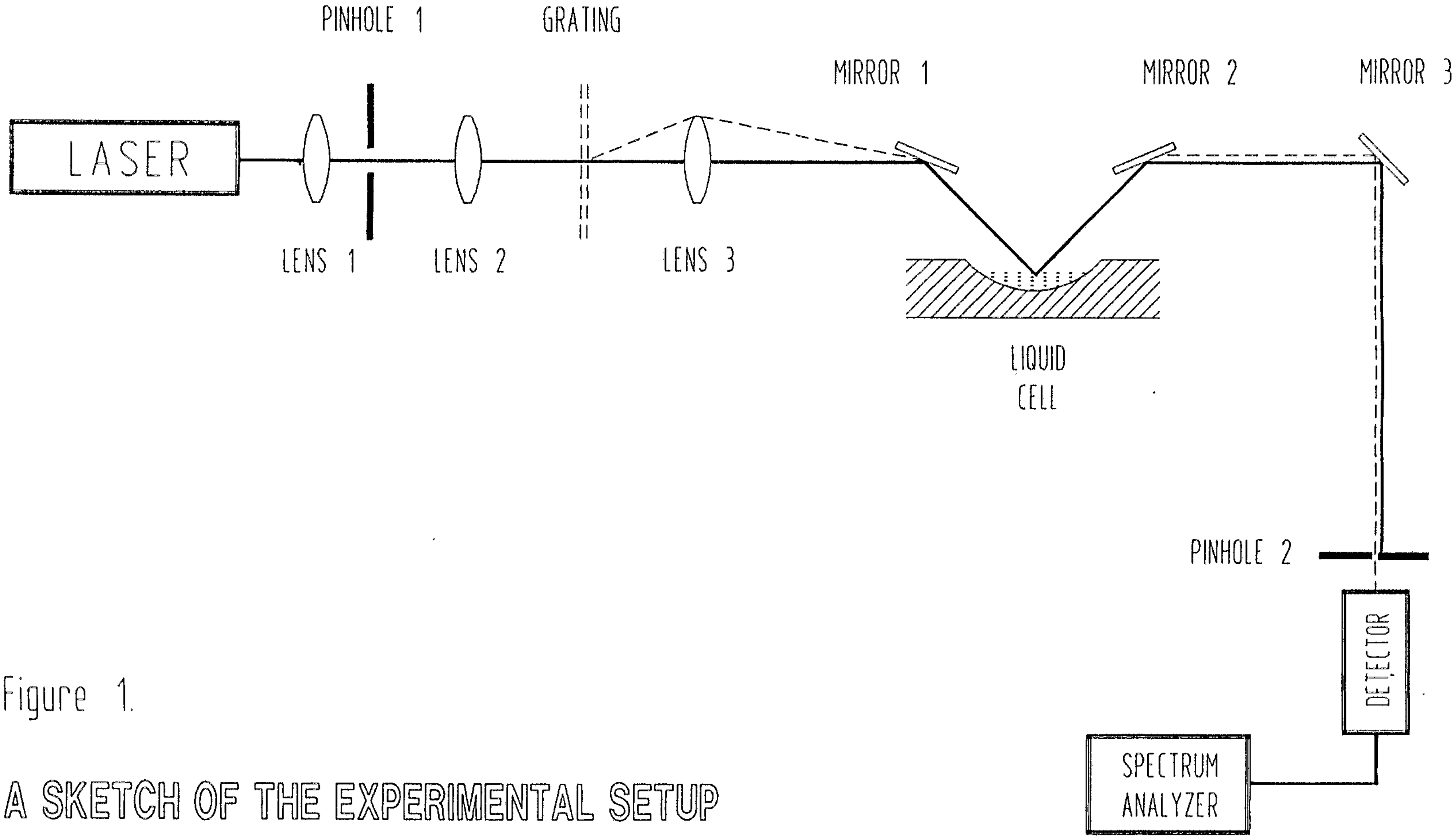

Figure 1.

A SKETCH OF THE EXPERIMENTAL SETUP

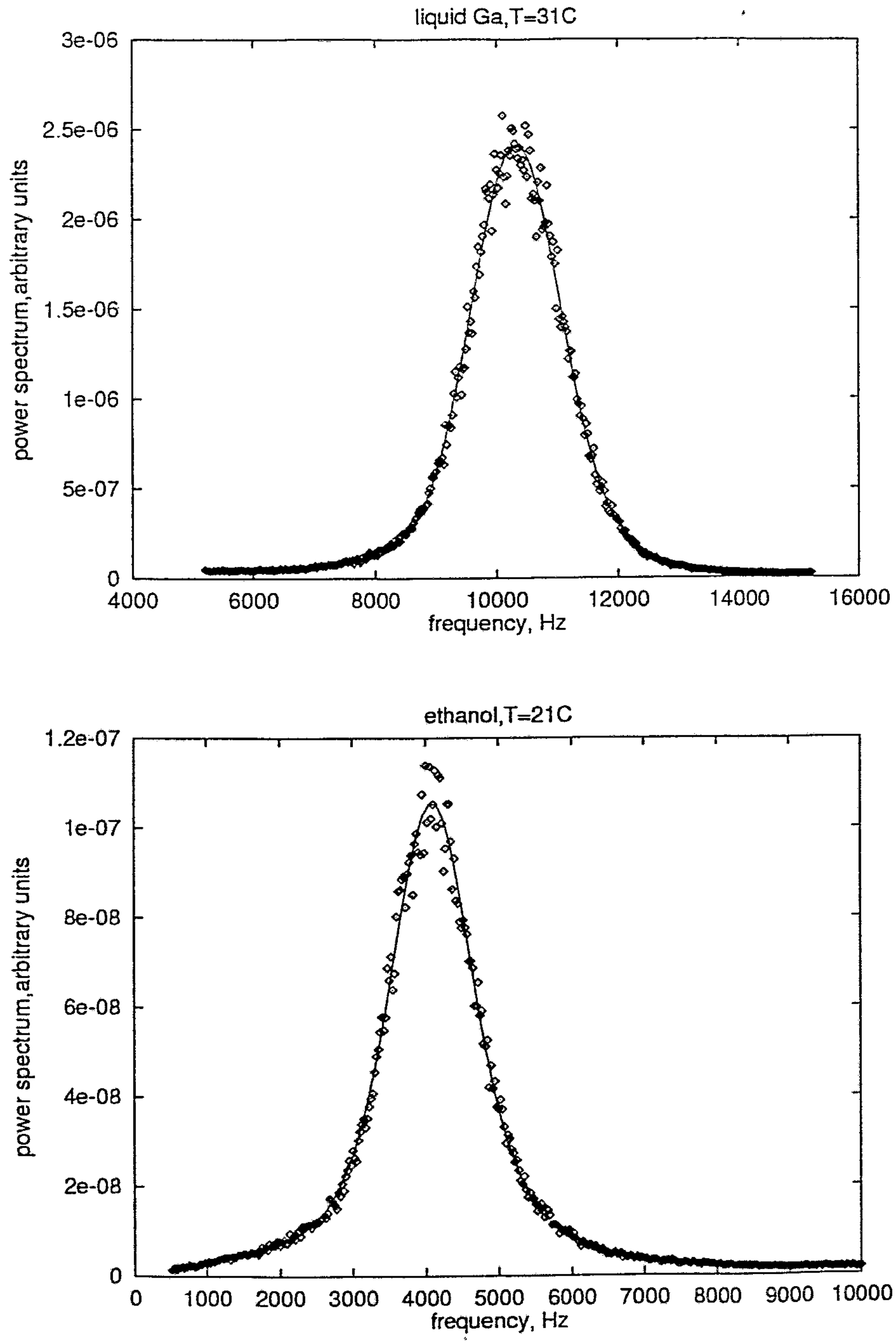

Figure 2: The power spectra of the light scattered by free surface of ethanol and Gallium. The solid line is fitting theoretical function in the form of (10).

3.1 Instrumental effects

The typical spectra are shown in Figure 2; the data were fitted with theoretical function which takes into account the effect of instrumental broadening: it arises from the illumination of more then one wave-vector q on the liquid surface; the spread δq in the wave-vectors gives a correspondent broadening in the frequency. A convolution between an ideal spectrum (3), having the Lorentzian shape and the Gaussian laser beam with a width β gives the theoretical form of the spectrum [14]

$$S(\omega) = A \cdot Re[exp(-\Gamma/\beta + (\omega - \omega_0)/\beta^2) \cdot erfc(-i\Gamma/\beta + (\omega - \omega_0)/\Gamma)] + B \qquad (10)$$

where A is a scaling amplitude, B is a background constant, and erfc denotes an error function of a complex argument. As it has been noted in [14] the ratio Γ/β is an increasing function of q. It means that an instrumental width should have a smaller effect at higher wavenumbers and deviations from the Lorentzian appear only at the wings of the spectra.

Using a nonlinear least-squares procedure the experimental data were fitted by the function $S(\omega)$. Unbiased estimates of ω_0 and Γ found from the spectra of the capillary waves on the surface of ethanol are shown in Fig.3 together with theoretical dependencies based on equation (2), (3) and well known physical properties of ethanol:

$\eta = 1.189 mPas, \gamma_0 = 22.7 mNm^{-1}, \rho = 789 kg/m^3$

The agreement between experimental data and theory seems to be nearly satisfactory, excepting the first point where deviations for Γ will be discussed below.

3.2 Heterodyne spectroscopy

The main problem of the detection process is the E_r/Es ratio. If it is too small the homodyne contribution is too strong; if it is too large the laser noise will dominate in the photocurrent.

Among the different sources of laser noise the most dangerous was the thermal broadband noise caused the fluctuations of the beam intensity displayed in form of long-periodic oscillations were able to ruin the spectrum quality. The amplitude of this noise does not exceed 0.5% of the laser intensity but it was sufficient to influence the measurements. The second type of noise arises from the power supply and displayed as a narrow peak around 40 kHz. This peak destroys the quality of the measured spectrum if the frequency of waves are found themselves near $40 \pm 10 kHz$. This peak has been suppressed with a LC-circuit, connected in parallel to the power supply.

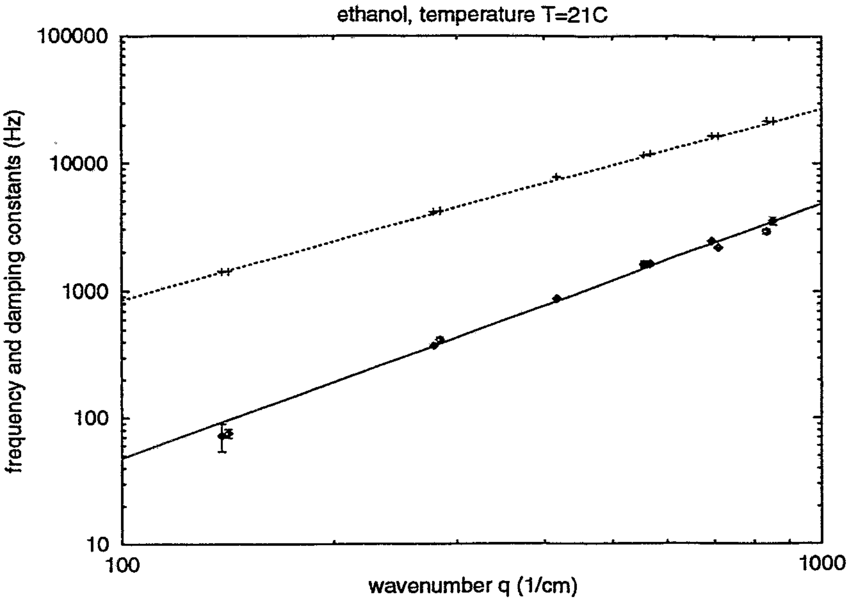

Figure 3: Peak frequencies+ and damping constants◇ of capillary waves at surface of ethanol. The lines are the solutions of the dispersion equation (1) and the properties of ethanol have their accepted values (see text).

The only one reliable way to escape the influence of laser noise is to decrease the intensity of the reference beam. It could be done in two ways : by choosing a "weaker" diffraction grating or by installing of an optical filter. Both ways are possible but the specific choice depends strongly on the type of the liquid sample, too. If the E_r/Es ratio is insufficiently large an additional peak at approximate twice frequency will appear in the measured spectrum. Fig. 4 illustrates this effect: the spectrum shown was obtained with a "weaker" grating than before. The result of fitting the spectra with sum of two functions, each in the form of (9) is shown with solid line. The deteriorated quality of fit is easily detectable in this case, where the fit gave much lower precision of estimation of the peak frequency and spectrum width.

Many researchers noted that mechanical vibrations were very harmful for the detection process. This observation is confirmed by the present study as well : despite the whole apparatus was placed on the optical table (Melles Griot), supplied with four air pressed cylinders (were mounted into the legs), the spectrum showed sometimes an inclined background which appeared due to vibrational disturbances. This can be accounted by using

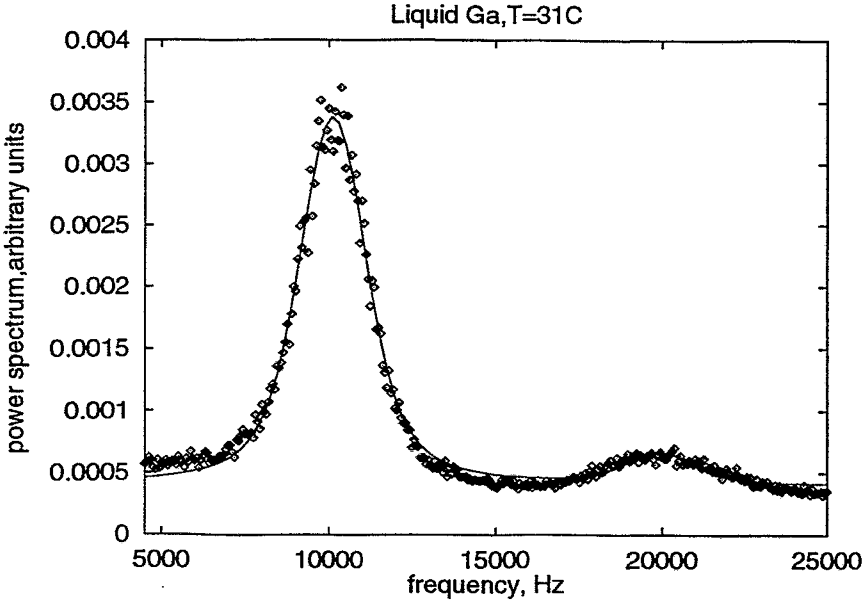

Figure 4: Power spectrum with contribution of homodyne term detected for liquid Ga at q=319.8 1/cm. The best fit to the data (see text) is shown with the solid line.

an appropriate form of the theoretical function.

3.3 Materials and sample cell design

Different kinds of liquid surfaces have been tested by means of capillary wave spectrometer: liquid Gallium and ethanol. In order to obtain clean free surface special care has been taken for the cleaning of the glass cell. It was found that a watch glass had the most suitable form: large scale disturbances were suppressed in the liquid placed in a container of such shape and secondly, it was easy to separate a satellite beam, appearing due to bottom reflection. The glass dish was mounted upon a copper plate supplied with water channels for thermostatic control. The cell was enclosed into a box made from organic glass with optical windows for the laser beam. The temperature of liquid was measured with a thermocouple, placed into the liquid.

In the case of liquid Ga a special container with optical window has been filled with Gallium using a sophisticated high-vacuum technique [15]. The main feature of this method was that working container has been filled with molten Ga from a pool using an "under the level" way of filling. In such a way an oxide skin remains in the pool and only pure Ga enters the recipient. The container had an outer diameter of about 70 mm and a height of 20 mm, was made from stainless steel and was sealed with a lead ring. Such sealing served really good against the gas from outside due to the strong contact (and even interdiffusion between deformed lead ring and glass surface). Container design and the presence of an U-shaped shutter filled with solidified gallium allowed to preserve a high vacuum without an extra vacuum pump: an adsorption getter pump, enable to maintain for-vacuum before the shutter tube. Heating or cooling was carried out from below through a copper plate drilled for an access of thermostatic controlled water. Temperature was measured with a very thin copper-konstantan thermocouple (diameter 0.2mm) glued to the container bottom. It has been supposed that in such a way measured temperature did not differ greatly from the true liquid metal temperature, because the thickness of the container bottom was rather small (0.5mm). The surface of Gallium has been free from contaminations during six month after preparation, nevertheless the presence of monomolecular film of Ga_2O_3 was not excluded (see below).

A main problem connected with Gallium was the surface curvature, despite the absence of visible meniscus near the container wall. Deviations from the flat surface appear due to the complicated wetting behavior of liquid Ga, fortunately the radius of curvature was many times larger than the size of the laser spot. The radius of curvature measured by means of the Schlieren optical technique was varying with radial position but the its smallest value was approx. 250 cm.

4 Direct spectral fit of the experimental data

The test measurements carried out at the surface of ethanol (Fig.3) gave results for the surface tension and viscosity which agree well with the theory based on the Dispersion Equation of capillary waves. Only for the q=151 cm^{-1} a poorer agreement must be related with an influence of the homodyne term on the spectrum [16]. However, for liquid Ga large discrepancies have been observed. The experimental results are shown in Fig.5 together with theoretical expectations. Different values of Γ for the same q were obtained by means of low-density optical filters installed without influence on the propagation of the main beam. The values of the peak frequency were biased from the theoretical dependence based on the surface tension data available from literature ($\gamma_0 = 724mNm^{-1}$),[17]. The fitting of the data with $\gamma_0 \sim q^{3/2}$ gave an unlikely high surface tension $\gamma_0 = 905 \pm 5mNm^{-1}$, though the character of $q^{3/2}$ variation is clearly displayed. The damping constants are greatly deviating from the theoretical line and no simple analytical expression (like q^2)

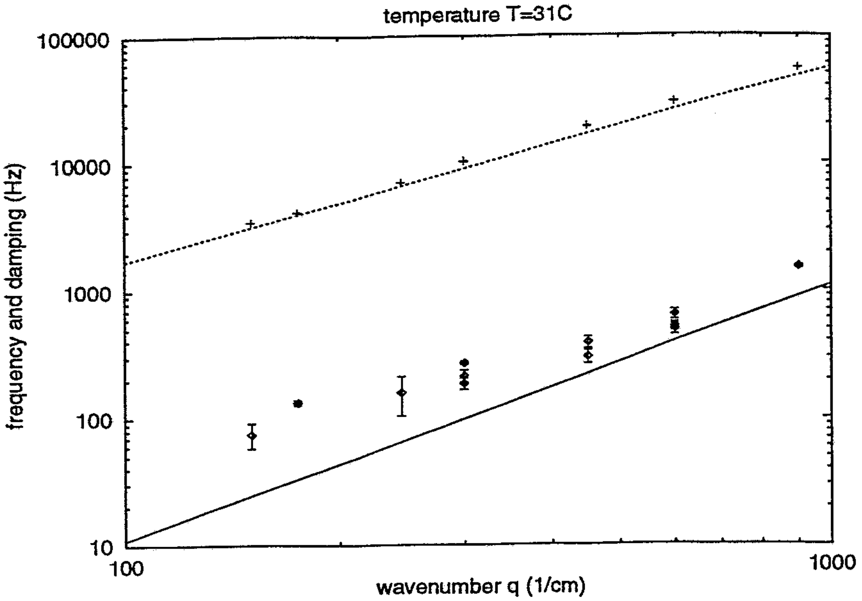

Figure 5: Peak frequencies+ and damping constants◇ of capillary waves at surface of liquid Gallium. The lines are the the theoretical predictions of the dispersion behavior based upon the following values of the physical properties of liquid Ga: $\gamma_0 = 724 mNm^{-1}, \eta = 2.08 mPa \cdot s, \rho = 6.09 kgm^{-3}$ Experimental point depicted for the same wavenumber were obtained by using different optical filters (see text).

can be proposed for describing of q-dependence.

Such anomalies in γ_0 and Γ can be explained only by the concept that the liquid metal surface is covered by a thin film of either molecules of metal oxide or, as was pointed out by [4], by a "monolayer" of neither metallic nor vaporised atoms. (We are not aware of the real thickness of the surface layer, therefore the word "monolayer" will be used only conditionally.) Such monolayer could be considered as compressible sheet with viscoelastic properties like those of organic surfactants. This complex situation can be described using two interfacial viscosities: shear γ', transverse to interface, and dilational ϵ' in the plane of interface, and the module of elasticity. Incorporation of these additional variables into the dispersion equation leads to drastic changes of Γ while the changes in ω_0 are only of minor importance. Some instructive examples of the effect of surface viscoelasticity on the propagation of capillary waves will be given here. Fig. 6 illustrates the influence of ϵ_0 on the frequencies and damping constants.

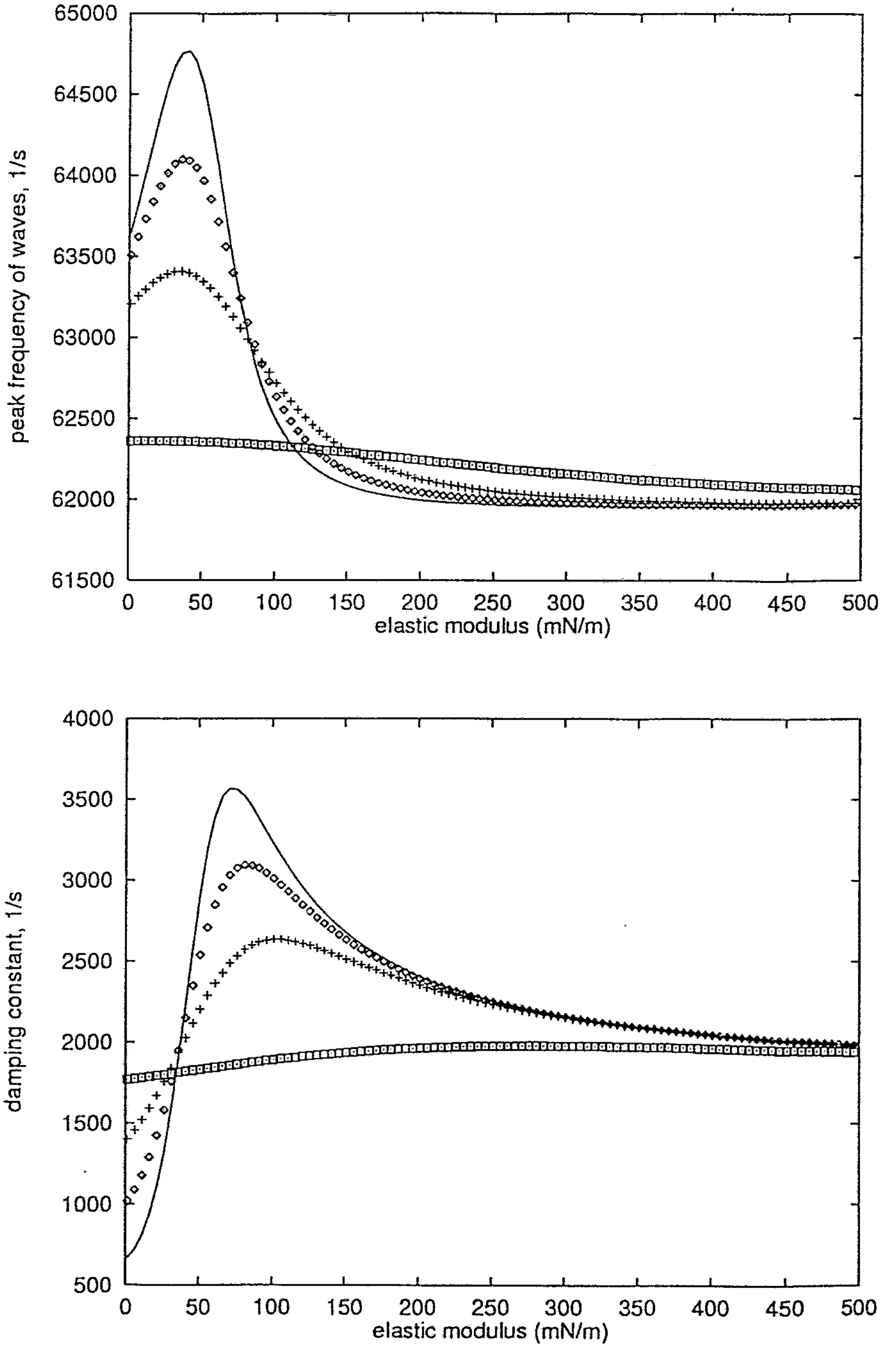

Figure 6.Frequencies and damping constants of capillary waves at a liquid Gallium surface with $\gamma_0 = 724mNm^{-1}$ as functions of ϵ_0 and ϵ' for $q = 310cm^{-1}$. The corresponding values of ϵ' are:$0(-), 2 \cdot 10^{-4}(\Diamond), 6 \cdot 10^{-4}(+), 4 \cdot 10^{-3}(\Box)(mNm^{-1}s); \gamma' = 0$.

A clearly visible hump proves an increasing of the damping near $\epsilon_0 = 70mN/m$; the further growth of ϵ_0 leads to the saturation. As has been expected the effect upon ω_0 is much weaker: the peak frequency changes only within 5% while the changes in Γ are from 4 to 5 times. Incorporation of the surface viscosity leads to the different behavior: variations in γ' from 0 to $4 \cdot 10^{-3} mN \cdot s/m$ amplify the damping while the same variations in ϵ' cause more complicated dependencies: when ϵ' rises ω_0 and Γ tend to be independent from ϵ_0.

It is possible to extract the values of viscoelastic properties from the spectra using many-parametric fit by the functional form where the four interfacial properties are involved. The main problem in fitting of real experimental data by Eq.(8) arises from the instrumental effect. In many of the earlier works, the researchers,dealing with the spectra, tried to neglect the instrumental broadening, what was correct for the liquids with high kinematic viscosity, or used indirect analysis of the experimental data. Such approach was found as lowering the accuracy of the considered technique. Thus the method of direct fit in the frequency domain, taking into account the instrumental effect, has been developed. The form of the autocorrelation function of the scattered light is [18]:

$$g(\tau) = FT[P(\omega)] \cdot exp(-\beta_* \tau/4) \tag{11}$$

if omitting some constant factors and second order terms. Here β_* is an instrumental width in some fictitious time domain defined by τ. It is the product of the Fourier transform (FT) of the power spectrum with instrumental term in the form of the Gaussian. Because actual "working space" is the frequency range the Fourier image of Eq.(11) has to be calculated:

$$\hat{P}(\omega) = \int_{-\infty}^{\infty} exp(i\omega t) g(t) dt \tag{12}$$

Thus, the Fourier Transform has to be applied two times: first to calculate the function $g(\tau)$ and second in the inverse direction to get the final form of the objective function. The data have been fitted by the functional calculated in 400 points:

$$F = \sum_{i=1}^{400} [P(\omega_i) - A \cdot \hat{P}(\omega_i, \gamma_0, \beta, \epsilon_0, \gamma', \epsilon')]^2 / \delta_i^2 \tag{13}$$

The function $\hat{P}$ represents the theoretical spectrum depending on 6 parameters: the four visco-elastic properties, instrumental width and an amplitude factor A ; it is our objective function. Because the values of the errors of experimental point δ_i were unknown we have used fit with equal weighting.

The fitting with the objective function in the form of (13) requires a strongly nonlinear minimization method. Levenberg-Marquardt method (Numerical Recipies in FORTRAN) has been used which is well established for practical applications and has become standard of nonlinear least-square program. The routine requires analytical expressions for derivatives and is based on the quasi-Newton algorithm for searching a minimum of a many variables function. Some acceleration factor was used: if F was far away from minimum the step in parameter space has been larger and smaller near the minimum. The calculations were performed in double precision and with the proper scaling of the fitted parameters. An unbiased estimated of the variance of the i-th parameter in the solution $\overline{x_i}$ is

$$var\overline{x_i} = \frac{2F_{min}}{p-N} H_{ii} \tag{14}$$

where p-is the number of free parameters, N- the number of points and H_{ij} is the Hessian matrix. The errors on fitted parameters have been estimated for 68.8 % confidence interval, using the so-called t-distribution with p-N degrees of freedom (NAG library).

Because the explicit equation connecting ω_0 and Γ with the four viscoelastic parameters is absent it is necessary to have an additional knowledge of the values of some of these parameters (in order of magnitude, at least). This information for a liquid metal interface is not available up to now in distinction from the monolayer on water surface have been studied by light scattering technique (for example [1]). All these studies were performed by spreading an expanded monolayer and monitoring the changes in light scattering spectrum during the monolayer compression. Some hints on the magnitudes of γ_0 and ϵ_0 can be obtained by this mean using the so-called surface isotherm where the values of the surface pressure versus molecular areas are presented. Such a technique is hardy imaginable for liquid Ga surface under high vacuum. Thus, the analysis had to be done in somehow restricted conditions without even approximate information on the ratio γ_0/ϵ_0 and only single value of surface coverage. The surface of liquid Gallium in the vacuum container was mirror reflecting without any visible traces of contamination. The monolayer on the surface was not "solid", its compressibility in the direction along the interface differed from zero, therefore the condition $\epsilon_0 << \gamma_0$ was expected. Recent papers show that two types of oscillations are present at a liquid interface: transverse and longitudinal (the second are driven by the local gradients of γ_0 along the interface). An additional hint for an estimation of the value of ϵ_0 could be obtained from the reasonable assumption that a maximal interaction between them appears if two surface modes oscillate close to resonance. Note, that the fitted values of ϵ_0 were strongly dependent on the initial conditions: at some values more than 200mN/m the fit converges to unrealistic solutions. The result of the fit, with the best fit values of parameters, is shown in Figure 7 together with residuals containing the difference between the model function and observed experimental data in each point. The residuals illustrate the magnitude of the noise upon the data: typically it

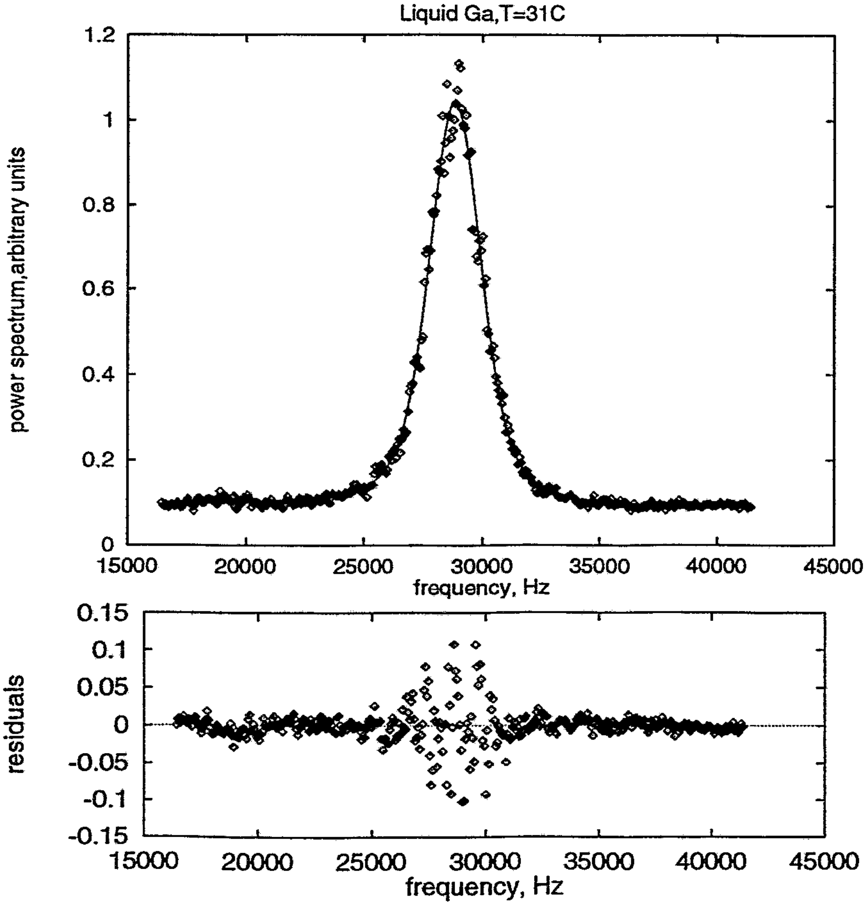

Figure 7: The best fit (shown with line) to the experimental spectrum at $q = 637.5cm^{-1}$. The fitted values of visco-elastic parameters are: $\gamma_0 = 723.6mNm^{-1}, \epsilon_0 = 22.78mN/m, \epsilon' = -1.36 \cdot 10^{-4} mN \cdot s \cdot m^{-1}, \gamma' = 1.99 \cdot 10^{-4} mN \cdot s \cdot m^{-1}$

was about 15-20% for nearly all the spectra. Nevertheless the residuals of the fit appeared uncorrelated and non-biased, demonstrating the adequacy of the model function. The obtained value of $\epsilon_0 = 22mNm^{-1}$, indicated that the surface film has been in rather liquid or expanded state, but it is difficult to comment this result in the absence of an adsorption isotherm (if such an isotherm is possible to obtain at all). The fitted values of the four surface properties are shown in Table 1.

Table 1. Visco-elastic properties from the direct fit of experimental spectra.

q, 1/cm	$\gamma_0, mN/m$	$\epsilon, mN/m$	$\epsilon', mN\cdot s/m$	$\gamma', mN\cdot s/m$
319	752 ± 6.2	22.2 ± 2.6	$(-1.83 \pm 0.9)10^{-4}$	$(4.2 \pm 1.8)10^{-4}$
319	756 ± 5.5	19.85 ± 2	$(-1.8 \pm 0.96)10^{-4}$	$(4.33 \pm 1.8)10^{-4}$
319	737 ± 3	17.9 ± 1.5	$(-2.5 \pm 0.25)10^{-4}$	$(6.7 \pm 0.85)10^{-4}$
482	745.3 ± 10.5	20.6 ± 3	$(-1.95 \pm 0.48)10^{-4}$	$(1.3 \pm 0.25)10^{-4}$
482	723.9 ± 6.7	24.3 ± 1.5	$(-2.29 \pm 0.2)10^{-4}$	$(4.36 \pm 0.9)10^{-4}$
685	723.6 ± 7.5	22.8 ± 2.1	$(-1.36 \pm 0.25)10^{-4}$	$(1.99 \pm 0.63)10^{-4}$

Various values of the surface properties obtained at the same q are corresponding to different I_r/I_s ratios. Magnitudes of two surface viscosities were self-consistent for all q and the dispersions were less than the central estimates for all parameters.

For the surface tension a gap between the literature data and its fitted values was found: γ_0 depends strongly on the surface condition: it could be underestimated if an oxide film covers the surface. The literature data for liquid gallium at $30°C$ scatter slightly: from 710 to 724 mNm^{-1} (Keene,1994). Note that the last value was obtained by using the method of pendant drop, where a drop of molten metal hangs freely at the end of a capillary-the thick skin of oxide was teared and the metal surface was in nearly free conditions. The values of the surface viscosities, inferred from the fit, appeared unexpected higher than those for a classical surfactant monolayer. The transverse shear viscosity has been always 3-4 times higher than that of the dilational viscosity. This could be an indication of the space properties of a film: it was easily compressible in plane of interface and hardly in direction normal to it. γ' might also be connected with relaxation processes in monolayer, as it has been shown in [19] for lipid monolayer.

5 Surface viscosity and waves destabilization

The value of the surface dilational viscosity has been found negative, independent of the initial guess and for all q studied. This strange phenomenon has already been detected for soluble monolayer of organic molecules on water and the linkage between $\epsilon' < 0$ and the mixing behavior of the surface modes has been revealed in [20, 21]. Following the ideas of the Belfast group one must return to the Dispersion equation in order to study its numerical solutions for the case of liquid Ga. Different values of the dilational viscosity correspond to different behavior of capillary and dilational modes. The waves are weakly coupled for zero or small negative value of ϵ' what is displayed in damping constants: Γ of the dilational mode is much higher than that of the capillary one. An increasing of $|\epsilon'|$ leads to the approaching of the damping constants and mode mixing occurs. The most interesting features can be obtained from q-dependence of a system of coupled oscillators. The behavior of two surface modes is shown in Fig.8 where the frequencies and temporal dampings for dilational and capillary modes are plotted using the values of viscoelastic parameters extracted from the fit. The coupled behavior turns into the mixed one (near $q \approx 1000cm^{-1}$) where the temporal damping of the capillary mode rises, but at the same time Γ of the dilational mode falls to negative values. The decrease of Γ is due to the negative ϵ'; the dilational wave damping is influenced mainly by ϵ' at higher q. Thus, between $q \approx 1000$ and $1500cm^{-1}$ dilational mode becomes capillary due to the mode mixing and oscillates with essentially negative Γ (is not shown). At the same time ω_0 is

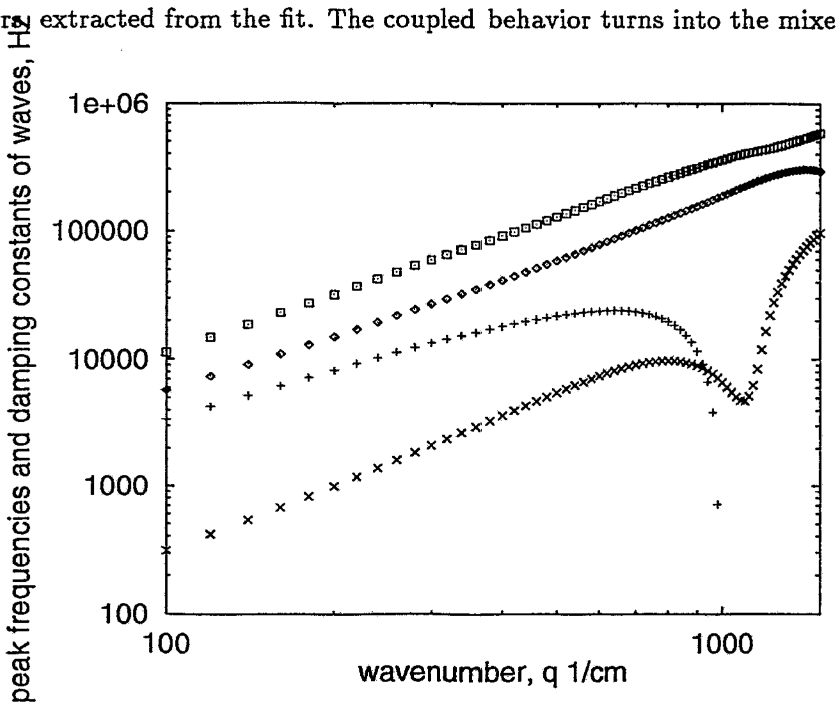

Figure 8: Coupled behavior of capillary and dilational waves on liquid surface with following properties: $\gamma_0 = 776mNm^{-1}, \epsilon_0 = 24mN/m, \epsilon' = -1.4 \cdot 10^{-4}mN \cdot s \cdot m^{-1}, \gamma' = 4 \cdot 10^{-4}mN \cdot s \cdot m^{-1}$. Damping constants of capillary mode are shown with $\times$, Γ of dilational with $+$. Peak frequencies of capillary mode are shown with $\Box$, ω_0 of dilational with $\Diamond$.

mixing and oscillates with essentially negative Γ (is not shown). At the same time ω_0 is growing up to a point at $q = 1200$ and falling down to zero at $q = 1600 cm^{-1}$ (not shown). So a consistent instability and overdamping of the dilational mode, caused by the negative ϵ' is clearly the case here.

It should be borne in mind, that the negative damping appears as a result of an application of the linear theory to the solution of the Navier- Stokes equation which is strictly non-linear. So one rather straightforward conclusion can be that as far as negative Γ has been obtained the linear theory does not valid any more: the negative damping leads to an exponential raising of waves amplitude. This fact seems to be difficult to check, because the dilational waves barely scatter light. Another explanation of the negativity of Γ might be that some additional physical processes like diffusive exchange between surface and bulk are responsible for the reduction of stability of the dilational mode. However the influence of diffusion or adsorption cannot be simply accounted for in the frame of the present theoretical model. Thus as has been already mentioned in [20, 21] the four surface properties are extracted from fitting the data by an inappropriate spectral form, so one may speak about "effective" values of the surface parameters, in particular ϵ' and ϵ_0. Unfortunately a theoretical spectrum of the surface waves influenced by all processes mentioned above is not available yet, nevertheless a plausible picture of two coupled modes at liquid surface will be given here. A hydrodynamical interpretation can be obtained from the more attentive view on the Dispersion equation, written into dimensional form [5, 18]:

$$[(\epsilon_0 + i\omega\epsilon')q^2 - i\omega(m+q)][(\gamma_0 + i\omega\gamma')q^2 - i\omega\eta(m+q) - \omega^2\rho/q] = -\omega^2\eta^2(m-q)^2 \quad (15)$$

All parameters have their usual meaning and $m = \sqrt{q^2 + i\omega\rho/q}$. This is a typical equation for two coupled oscillators, where the right hand side is a coupling constant, the first bracket on the left side describes the dilational mode the second one-the capillary mode. Coupling between them is realized via viscosity that reflects the possibility of generation a longitudinal wave during the passage of a capillary one. The frequency dependence of the coupling constant is indicating that the longitudinal wave generates pressure gradients (due to inertia of the liquid) being able to cast into the transverse wave. When q and frequency growth ϵ' is making the damping of dilational wave negative. For some q in the range $900 < q < 1600 cm^{-1}$ this mode converts into the capillary type (mainly) and becomes overdamped for $q \approx 1600 cm^{-1}$ while the second mode, being initially of capillary type, switches to longitudinal one. This transition is mostly apparent in the behavior of damping constant of capillary mode which undergoes rapid variations at $900 < q < 1200 cm^{-1}$. Such variations, if they are really existing, should be detectable in light scattering experiment.

Unfortunately the resolution of the spectrometer did not allow to collect reliable results for $q > 10001/cm$ and an additional investigation is thus strongly required.

This complicated wave behavior might be explained in terms of hydrodynamics by decrease of the "effective" bulk viscosity: the thickness of the hydrodynamic boundary layer created by the high frequency longitudinal stresses at the surface of the fluid drops due to reduced bulk viscosity and the pressure gradients normal to the surface become insufficient to sustain the transverse wave. The following scenario of events can be proposed: mode mixing makes the dilational mode of capillary type, which means that the transverse oscillations are generated mainly by the oscillatory horizontal component of the applied stress. But these oscillations are out of phase: under some value of the phase shift the horizontal force is not able to create any significant motion necessary to sustain the transverse wave, this wave becomes overdamped. Only "capillary" mode remains, but it looks now like "dilational" one. Of course the explanation given here has an approximative character: for a more exact description of this complicated coupled behavior information about the relative magnitude of wave amplitudes is strongly required.

6 Diffusion, adsorption and surface viscoelasticity

Light scattering experiment has been repeated in order to get more reliable results especially at high wavenumbers. Unbiased estimates of peak frequencies and damping have been obtained after the first stage of the data evaluations undertaken exactly in the same manner as it has been described already. The results are shown in Fig.9 together with the theoretical q-dependencies for liquid Ga surface as a "simple fluid". Different values of Γ for the same q have been derived for various I_r/I_s ratios, by making use of filters with varying optical density. While for peak frequencies the deviations from theoretical predictions are negligible, the large anomalies for Γ remain evident, especially for $q < 500cm^{-1}$. At the second stage the values of the surface viscosities were inferred by means of a fit of experimental spectra with the well-known theoretical form [18, 1]. The negative values of the dilational viscosity ϵ' have been found again for all wave-numbers while the errors on the parameters were less than central estimates returned by the fit. These results were self-consistent over the whole q-range.

The explanation of the negativity of dilational viscosity and following from it surface waves destabilization [19] seems to be disputing due to an absence of an explicit source of energy for disturbances growth. I do not want to diminish the significance of the basic theory, but note that an essential shortcoming of the theoretical model was that no connection

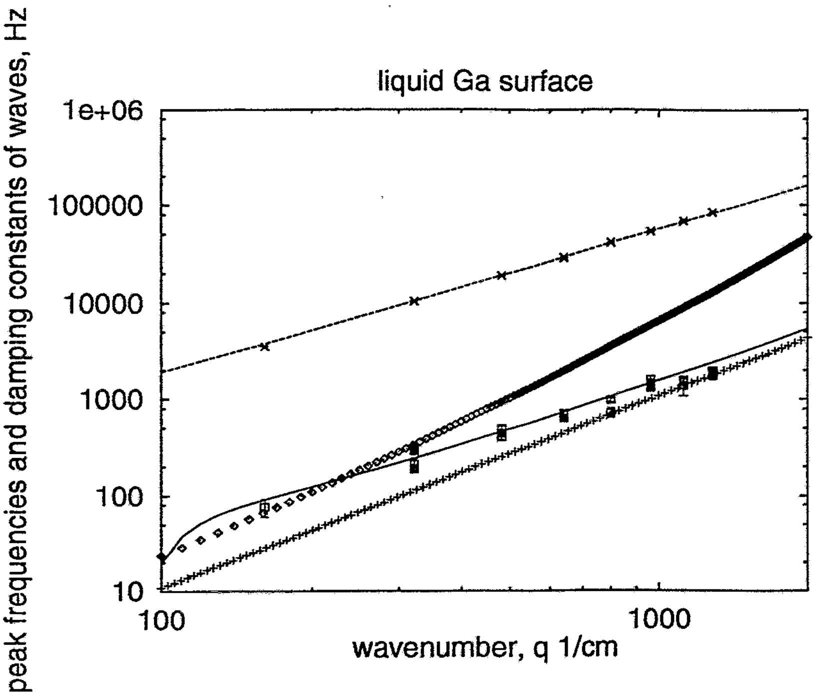

Figure 9: Experimental data for frequencies × and damping constants □ of capillary waves at the surface of liquid Ga. The theoretical predictions for ω_0 are shown with dotted line and Γ-with $+$, as for the free surface of liquid Ga with well accepted surface and bulk properties (see text). The theoretical variations of Γ for liquid Ga interface with $\epsilon_0 = 20mNm^{-1}, D = 2 \cdot 10^{-4}cm^2/s, a/\Gamma_\infty = 2 \cdot 10^7 1/cm, \gamma_0 = 750mN/m$ are depicted with ◇ for $\gamma' = 4 \cdot 10^{-4}mNsm^{-1}$. Solid line represents the theoretical variations of damping constant for the case of $a/\Gamma_\infty = -2 \cdot 10^7 1/cm, \gamma' = 0, D = 2 \cdot 10^{-4}cm^2/s, \epsilon = 20mNm^{-1}, \gamma_0 = 750mN/m$.

of the surface viscosities with other physical variables has been established. Therefore, one may turn to the old but rather important papers [22, 9] where the main equations of mass transfer on fluid-monolayer interface have been written for the most interesting case of soluble monolayers. The complex module ϵ has been linked there to the solute transfer, influencing the local equilibrium between the surface and the concentrational boundary layer. An important point is that the quasi-equilibrium between the concentration in a sublayer and the local values of γ_0 and Γ_s directly on the surface is assumed. Using this central assumption, ϵ may be regarded as an equilibrium property, connecting the changes in surface tension and changes in area A: $\epsilon = \frac{d\gamma_0}{dln\Gamma_s}\frac{dln\Gamma_s}{dlnA}$. In the case of soluble surfactants the equation of mass balance requires that variations of the surface coverage Γ_s due to the passage of longitudinal wave are balanced by diffusion of solute from the bulk, if the surface diffusion is negligibly small.

$$\begin{aligned} \frac{d(\Gamma_s A)}{dt} + AD(\frac{dC}{dz})_s &= 0 & (16) \\ \frac{dC}{dt} - \vec{V}\nabla C &= D\Delta C & (17) \end{aligned}$$

The general solution of the diffusion equation was taken in the form of a product between the wave oscillating in time with complex frequency ω, propagating along the interface with wavenumber q and exponentially damped (along z) term with penetration depth n: $C \sim C_0 exp(nz) exp[i(qx + \omega t)]$. If only the waves of small amplitude are considered and the convective term in the equation of diffusion is neglected, then the expression for complex dilational modulus appears in the form:

$$\epsilon = \frac{\epsilon_0 \omega}{\omega - inD\frac{dC}{d\Gamma_s}} \qquad (18)$$

where $n = \sqrt{q^2 + i\omega/D}$ and ϵ_0 is the real dilational modulus, having the same form as for insoluble monolayers: $\epsilon_0 = -\frac{d\gamma_0}{d\Gamma_s}$. In [22] (18) has been written for real ω for the case of externally excited waves but the present idea is to use complex form of $\omega = \omega_0 + i\Gamma$ for the waves with non-zero temporal damping. The inclusion of $\frac{dC}{d\Gamma}$ into the model implies the existence of quasi-equilibrium between the time-averaged surface property Γ_s and bulk concentration C. The term $\frac{dC}{d\Gamma}$ expresses the slope of the so-called adsorption isotherm, which could be found from the form of the Langmuir isotherm, taken for the sake of simplicity:

$$\frac{dC}{d\Gamma_s} = \frac{(C/a + 1)^2 a}{\Gamma_\infty}, \qquad (19)$$

where Γ_∞ is the surface saturation concentration and a is the bulk concentration corresponding to the surface adsorption of $\Gamma_\infty/2$.

7 Numerical solutions of the modified Dispersion Equation

After the substitution of the complex form of ϵ into the dispersion equation (15), it can be written as:

$$[\omega\epsilon q^2 + i\omega(\omega - inD\frac{dC}{d\Gamma_s})\eta(m+q)][\gamma q^2 + i\omega\eta(m+q) - \omega^2\rho/q] = -\omega^2(\omega - inD\frac{dC}{d\Gamma_s})[\eta(q-m)]^2 \qquad (20)$$

Now the coupling constant on the right hand side contains not only bulk viscosity but also the diffusional and adsorption terms. A numerical solution of (20) is shown in Figure 10.

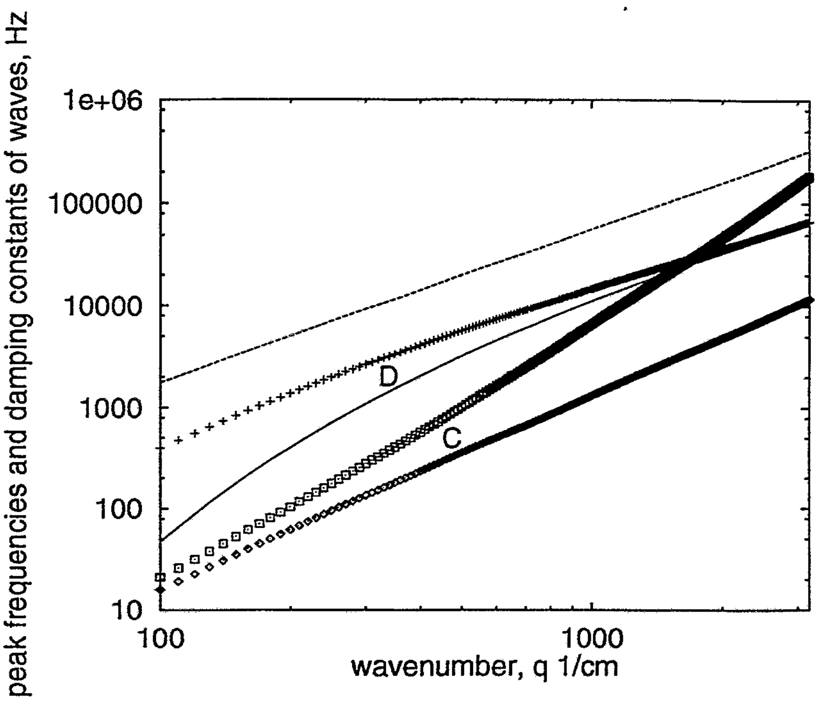

Figure 10: Frequencies and dampings for coupled capillary, denoted C and dilational waves D on the liquid surface with properties: $\gamma_0 = 750mN/m, \epsilon_0 = 20mN/m, D = 2 \cdot 10^{-4}cm^2/s, a/\Gamma_\infty = 5 \cdot 10^7 1/cm, \gamma' = 0$. ω_0 of both modes are shown with solid and dotted lines, Γ with $+$ for dilational wave and with $\diamond$ for capillary one. Variation of Γ of capillary mode for $\gamma' = 410^{-4}$ is depicted with $\square$ and discussed in the text.

For the case of $\gamma' = 0$ it demonstrates the weak-coupled modes behavior found for all values of D and a/Γ_∞ over the range $1 \cdot 10^{-5} < D < 1 \cdot 10^{-3}(cm^2/s)$ and $1 < a/\Gamma_\infty < 1 \cdot 10^7(1/cm)$. The mode coupling appears to be somewhat one-sided: the dilational mode has a strong influence on Γ of capillary one while the latter barely effects the former. The variations of ϵ_0 may cause the frequency resonance between capillary and dilational modes, but did not change the principal behavior of Γ for both modes. With increase of D the longitudinal mode behavior is very similar to the pure uncoupled case and for $D > 2 \cdot 10^{-3}cm^2/s$ the longitudinal mode is overdamped for $q < 200cm^{-1}$, but it is unlikely, that the diffusion coefficient could be so high.

Under some $a/\Gamma_\infty > 1 \cdot 10^7 1/cm$ the dispersion behavior of longitudinal waves differs from the well known solution (see, for example, [21]). If a/Γ_∞ rises further, the surface viscosity is not negligible and the damping becomes equal to the peak frequency, and for $q < 500cm^{-1}$ even exceeds the latter. Now the purely dilational mode is looking like a wave might be called a concentrational one which tends to become overdamped with growth of a/Γ_∞. This behavior may be understood from the physics of propagation of dilational waves. Increasing the concentration of solute in the bulk leads to the appearance of the diffusional boundary layer just beneath the surface. If the concentration gradients in this layer are high enough, then the diffusion (as well as adsorption) suppresses the gradients parallel to the surface. This means, that in the limit of very high concentration nothing of the visco-elastic behavior will remain- the surface tension gradients are "short circuited" by the fast adsorption processes and the surface looks like a "free" surface, but with higher bulk viscosity. The role of diffusion as well as adsorption is to amplify the effective viscosity of the interface that, in turn, causes a rapid decrease of ω_0 and Γ of dilational mode, but the equality $\Gamma_l = \Gamma_c$ is never achieved, due to the overdamping of concentrational wave. This seems to be the main reason why the diffusion and adsorption as well play rather minor role in the mode mixing. Strongly coupled solution of (20) for the nonzero γ' is shown in Figure 10 as well. In this case the modes mixing has been predicted in [21], but without considering of any diffusion-adsorption processes. The principal character of dependencies is not changed in this case by variations of D up to $1 \cdot 10^{-3} cm^2/s$-above this value the dilational wave is overdamped exactly in the same manner as has been considered above. Note, that only the γ' provides the effect of approaching the damping coefficients of the modes in such a way that above $q = 1000 cm^{-1}$, for particular ϵ_0, neither capillary nor dilational behavior can be distinguished.

One can see a contradiction between the reported q-dependence and the results of the fit. Indeed, it is well-known [20, 21] fact that the negative ϵ' leads to very strong coupling and mixing between two surface modes, what is not reflected in the outlined theory. Therefore, one must recall that Γ_s into the adsorption isotherm is the surface excess concentration which might, in principal, be negative. Then the dispersion behavior is changed drastically: a tendency in wave mixing is visible below $a/\Gamma_\infty = -5 \cdot 10^6 1/cm$. In the case of $\Gamma_s < 0$ one can speak about the surface deficiency concentration instead of the surface excess. The variations in ω_0 and Γ are shown in Figure 11. At high q ($q > 500 cm^{-1}$) the frequencies of capillary and dilational wave follow approximately the "normal" q-dependence but below ($q \approx 200 cm^{-1}$) the modes can not be distinguished between each other, so that complete mixing is apparent. Note, the experimental Γ observations are best-matched to the theoretical damping curves of capillary mode for the case of $\gamma' = 0, a/\Gamma_\infty = -2 \cdot 10^7$ (see Figure 9). The value of the dilational viscosity can be estimated as: $\epsilon' = [Im\epsilon]/\omega_0$, where ϵ is given by (19). ϵ' calculated in such a way is negative for all

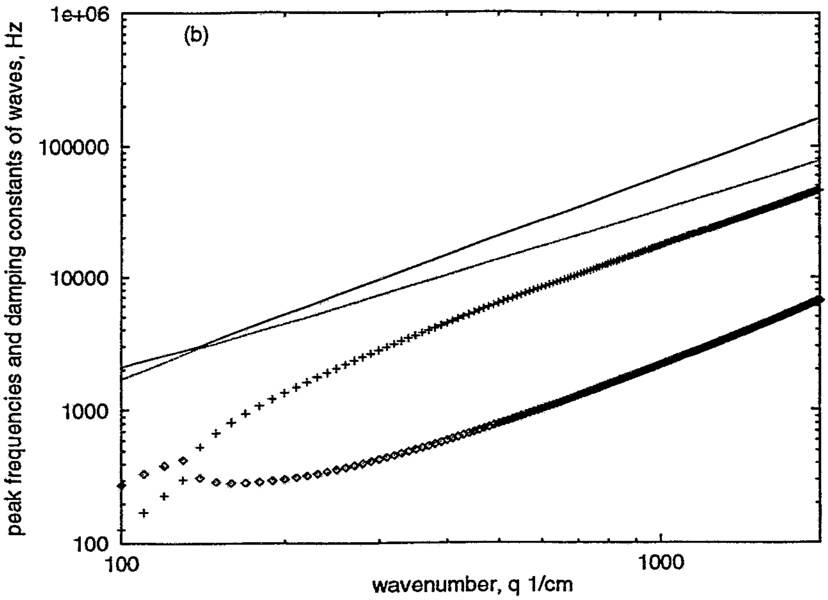

Figure 11: Frequencies and damping values for strongly coupled modes on the liquid surface with the following properties: $\gamma_0 = 750mN/m, \epsilon_0 = 29mN/m, D = 2 \cdot 10^{-4}cm^2/s, a/\Gamma_\infty = -2 \cdot 10^7 1/cm, \gamma' = 0$. The solid and dotted lines correspond to ω_0 of both waves. Variations of Γ of dilational-like wave are shown with $\diamond$ and Γ of capillary-like with $+$.

q over the range $100 < q < 2000(cm^{-1})$.

8 Conclusions

This work demonstrates that light scattering from thermally exited capillary waves can be unique inexpensive technique (in comparison with X-ray scattering) for yielding information about surface properties of molten metals. If the problem with instrumental broadening is solved the evaluation of light scattering data will give unbiased estimates for ω_0 and Γ of the surface capillary waves. In the first stage we found that the physical properties of the liquid Ga surface differed from postulated in the Handbook values. Especially great anomalies were found for the damping coefficient of the surface capillary waves with respect to the assumption that these waves propagate on free surface of liquid Ga. This result resembles the earlier observations of the free surface of mercury [3, 4].

A reasonable assumption about the presence of a monolayer, possessing four visco-elastic properties has been made and a successive attempt to extract these parameters has been undertaken. Direct analysis of spectra of scattered light has been done in the frequency domain, though the most successive earlier attempts were made in the time domain. The sensitivity of the method is maximal to the viscoelastic modulus and the surface tension; the values of the surface viscosities are extracted with greater fractional errors. The method of direct fitting, being insensitive to the starting point, does not require *a priory* knowledge of relations between the parameters and directly measurable ω_0, Γ. A highly reproducible negative value of the dilational viscosity has been obtained which was found up to now for completely different water-like systems covered with a monolayer.

The dispersion behavior can be understood in terms of strong coupling and even mixing between capillary and dilational modes which seems to be an intrinsic property of a liquid, supporting a soluble monolayer. Some doubts still remain whether the negative dilational surface viscosity really exist or its negativity reflects incomplete understanding of all physical processes influencing the wave propagation at the interface. Indeed, the chemical adsorption-desorption processes have not been accounted for into the scattered light spectrum, but in fact they are very important in a liquid metal surface occurring in the dynamic equilibrium with the bulk. Therefore an attempt to find a link between kinetics of adsorption and surface viscoelasticity has been undertaken. Present simulations have rather approximative character; indeed, it seems to be impossible to hold one or two parameters fixed over the whole q-range, but one feature can be outlined definitely: for $a/\Gamma_\infty > 0$ no region where one of the two modes was unstable has been found. For $a/\Gamma_\infty < -7 \cdot 10^7$ (for particular $D = 2 \cdot 10^{-4} cm^2/s$) one can find a q-range where the damping values of the capillary wave have been negative what points out on the wave instability. The real existence of such values of the diffusion coefficient and the surface concentration is questionable up to now. The form of equation for the absorption isotherm is not well-established for liquid metals. It was shown in [23] that the presence of an adsorption barrier can reduce the stability of dilational waves. The consideration has been made for the uncoupled modes-which might be relevant to this case, accounting for a tendency of weak coupling at high q. However, the physical situation considered in [23] could not be directly transfered to the random surface waves: due to an absence of steady gradient of solute trough the interface, postulated in [23]. The role of this concentrational gradient should not be underestimated-under certain circumstances it can be a source of energy for the growth of disturbances. As far as a system does not exchange energy with the surroundings, there is no manifest reason for destabilization of the waves. Nevertheless, there is an intrinsic sublayer (thickness of a few atomic diameters) directly beneath the surface which was not accounted by the present model, a concentrational "jump" has been implied in the frame of hydrodynamic approach. Perhaps calculations of the interfacial kinetics, included into the theoretical model, would finally clarify the question of the surface modes instability.

Acknowledgments

Financial support from the German Space Agency (DARA) as well as German-Israeli Foundation is gratefully acknowledged. Fruitful discussion was sheared with J.Priede (*Forschungszentrum Rossendorf*).

References

[1] Langevin D.(Ed.) 1992 Light scattering by liquid surfaces and complementary technique. Dekker, New York

[2] Earnshaw J C and R C McGivern 1987. J.Phys. D:Appl. Phys. 20 82-92

[3] Bird M and Hils G 1977 in Physicochemical Hydrodynamics vol 2, ed. D. Spalding (London: Advance) p.609

[4] Earnshaw J.C. 1982 Physics Letters 18, 40

[5] Kramer L. 1971 J. Chem. Phys. 55, 5 2097-2105

[6] Sluis D., D'Evelin M.P. and Rice S.A. 1982 J. Chem. Phys. 78(3), 1611

[7] Regan M.J.,Kawamoto E.H., Lee S., Pershan P.S.,Maskil N., Deutsch M., Magnussen O.M., Ocko B.M., Berman L.E. 1995 Phys. Rev. Lett. v.75,13, 2498

[8] Magnussen O.M., Ocko B.M.,Regan M.J.,Penanen K.,Pershan P.S., Deutsch M. 1995 Phys.Rev. Lett. v.74, 22, 4444

[9] Levich V.G. 1962 Physicochemical Hydrodynamics. Prentice Hall, New York

[10] F.C.Goodrich, Proc.R.Soc.London A 374, 341 (1981)

[11] H.Lamb, Hydrodynamics (Dower, New York, 1945), p.626

[12] Cummins H.G. 1974 in: Photon Correlation and Light Beating Spectroscopy. Plenum, New York

[13] Jorgensen T.M. 1982 Meas.Sci. Technol. 3, 588

[14] Hard S.,Hamnerus Y. and Nilsson 1976 J. Appl. Phys. 47,2433

[15] Bojarevich A., Gelfgat Yu.M., Gerberth G. 1994 in Proceeding of the Second International Conference on Energy Transfer in MagneHydroDynamic Flows, France, pp. 117-126

[16] Hughes C.J. and Earnshaw J.C. 1993 Rev. Sci. Insrum. 64(10), 2789

[17] Keene B.J. 1993 Inter.Mater.Rev. 38, 4, 157

[18] Earnshaw J C, McGivern R.C.,McLauhlin A.C. and Winch P.J. 1990 Langmuir 6, 649

[19] Earnshaw J.C., McGivern R.C and Winch P.J. 1988 J. Phys. France 49, 1271

[20] Earnshaw J.C. and McCoo E. 1994 Phys. Rev. Lett. v.72,1 84-87

[21] Earnshaw J.C. and A.C. McLaughlin 1993 Proc. R. Soc. Lond. A 440, 519-536

[22] E.H.Lucassen-Reynders and J.Lucassen, Adv.Colloid. Interface Sci. 2, 347 (1969)

[23] M.Hennenberg, X.-L. Chu, A.Sanfeld, and M.G.Velarde, J.Colloid Intrface Sci. 150,7 (1992)